Journal of Imaging Science and Technology® 63(6): 060404-1–060404-7, 2019.

Parameter Estimation of PuRet Algorithm for Managing Appearance of Material Objects on Display Devices

Midori Tanaka▲
College of Liberal Arts and Sciences, Chiba University, Chiba, Japan
E-mail: midori@chiba-u.jp

Ryusuke Arai and Takahiko Horiuchi▲
Graduate School of Engineering, Chiba University, Chiba, Japan

Abstract. *In addition to colors and shapes, factors of material appearance such as glossiness, translucency, and roughness are important for reproducing the realistic feeling of an image. In general, these perceptual qualities are often degraded when reproduced as a digital color image. The authors have aimed to edit the material appearance of an image as measured by a general camera and reproduce it on a general display device. In their previous study, the authors found that the pupil diameter decreases slightly when observing the surface properties of an object and proposed an algorithm called "PuRet" for enhancing the material appearance based on the physiological models of the pupil and retina. However, to obtain an accurate reproduction, it was necessary to manually adjust two types of adaptation parameters in PuRet as related to the retinal response for each scene and the particular characteristics of the display device. This study realizes the management of the appearance of material objects on display devices by automatically deriving the optimum parameters in PuRet from captured RAW image data. The results indicate that the authors succeeded in estimating an adaptation parameter from the median value of the scene luminance as estimated from a RAW image. They also succeeded in estimating another adaptation parameter from the average value of the scene luminance and the luminance contrast value of the output display device. As a result of an experiment using an unknown display device that was not applied to derive the estimation model, it was confirmed that the proposed model works properly.* © *2019 Society for Imaging Science and Technology.*
[DOI: 10.2352/J.ImagingSci.Technol.2019.63.6.060404]

1. INTRODUCTION

Imaging technology for reproducing appropriate appearance factors of a material, such as glossiness, translucency, and roughness, has recently become desirable for use in the color imaging industry [1, 2]. We have been faced with a major problem in that the material appearance obtained from actual objects and their images when rendered on different devices may not be equivalent. Such a visual difference is often a major problem when shopping on the Internet, and perceptually equivalent reproduction is required. Through psychophysical experiments, Tanaka et al. clarified the differences in perceptual qualities of a material appearance obtained from 34 actual objects, including ten material categories (stone, wood, metal, paper, fabric, plastic, leather, glass, ceramic, and rubber), and their images rendered using different reproductions as displayed on a monitor [3]. The results indicate that the reproduced images of certain materials significantly affect their perceptual quality.

Research on the reproduction of a material appearance has been conducted in the fields of engineering, vision and neuroscience, and psychophysics, among others. In recent years, realistic approaches to treating a material appearance with high fidelity or high favorability have succeeded in terms of their implementation in industrial applications. In the field of engineering, many different techniques for measuring the appearance of a material have been proposed during the last few years [4, 5], which have produced large public datasets used for accurate, data-driven appearance modeling [6]. However, although this has allowed us to reach an unprecedented level of realism in terms of visual appearance, editing the captured data remains a challenge. Some methods treat material editing as an image filtering problem. Khan et al. [7] utilize simple heuristics to infer approximate shape and illumination information from an image and utilize this knowledge to apply material editing. Boyadzhiev et al. [8] introduced several image filters to change certain properties such as the shininess and glossiness. Although these approaches achieve photo-realistic results, they provide limited editing scenarios.

In our previous study, we proposed a new image-processing algorithm called "PuRet" for enhancing the appearance of a material, such as glossiness, transparency, and roughness, obtained from digital color images [9]. Using this algorithm, we focused on changes to the pupil diameter and retinal response that are first handled in the human visual system to recognize an image. First, through a psychophysiological experiment, we measured the changes in pupil diameter of the observers before and after they focused on the material appearance of an object surface. Based on this experiment, it was found that the pupil diameter decreases when observing the material appearance on the surface of an object. Second, we designed a new algorithm for enhancing the perceived appearance of material by contracting the pupil diameter based on a retinal response model proposed by Naka and Rushton [10] and confirmed the effectiveness by applying the algorithm to general digital color images. There

▲ IS&T Members.

Received July 4, 2019; accepted for publication Oct. 10, 2019; published online Dec. 13, 2019. Associate Editor: Rita Hofmann-Sievert.
1062-3701/2019/63(6)/060404/7/$25.00

are two types of parameters used by PuRet depending on the adaptation level for the illumination, the adaptation level under careful observation and the adaptation level based on the display characteristics. These parameters should be optimized depending on the luminance level in a scene and the display characteristics. However, in [9], such parameters are manually adjusted, and optimum parameter tuning is therefore an important topic of future research.

In this study, a parameter estimation algorithm for managing the appearance of material objects shown on a display device was developed. In the field of vision and psychophysics, visual appearance has been studied as a type of "soft metrology" [11, 12]. The soft metrology concept was first introduced by Pointer in a National Physical Laboratory (NPL) report in 2003 [13] and was defined as the "measurement techniques and models which enable the objective quantification of properties determined by human perception." In the NPL report, Pointer highlights that soft metrology can be a key factor in industrial applications. In addition, the European community and the Commission Internationale de l'Éclairage (CIE) recognized [14, 15] soft metrology as a key to competitiveness. In this study, we follow the framework of soft metrology and estimate the parameters in PuRet through psychophysical experiments. We assume that RAW image data can be captured and that the camera characteristics are known in advance. First, we estimate the luminance adaptation level of a scene from a captured image. Then, for a master display device, we estimate an enhanced luminance adaptation level through careful observation of the image. Finally, for an arbitrary display device, we attempt to automatically estimate the parameters found during the careful observation. The feasibility of the proposed estimation model is verified using an unknown display device.

2. PuRet: MATERIAL APPEARANCE ENHANCEMENT ALGORITHM

In [9], we proposed the PuRet algorithm for enhancing the appearance of a material based on the measured pupil diameter. Figure 1 shows a schematic diagram of the concept used by PuRet. In general, digital color images captured by a camera are generated through various image-processing techniques based on the visual properties. Detailed algorithms applied in commercial cameras are considered black boxes. We focused on the retinal responses from light after passing through the pupil. As shown in the flow at the top of Fig. 1, a normal color image is generated regardless of changes to the pupil diameter. However, according to the new findings in [9], images with an enhanced material appearance must be generated by assuming that the scene acquisition occurs under a contracted pupil size, as shown in the bottom flow of Fig. 1. We converted a normally processed JPEG image into an enhanced image using the conversion function φ.

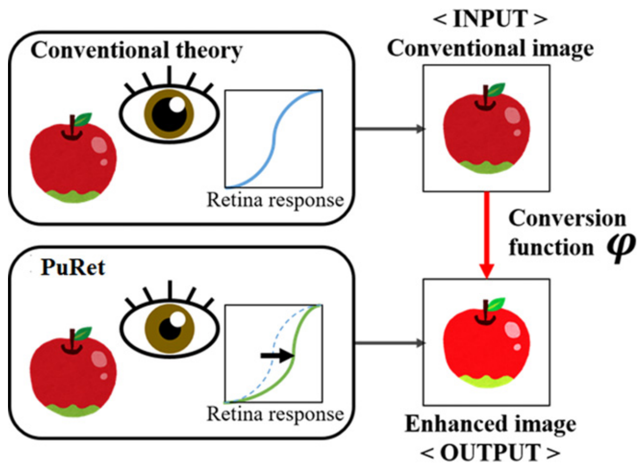

Figure 1. Concept of PuRet.

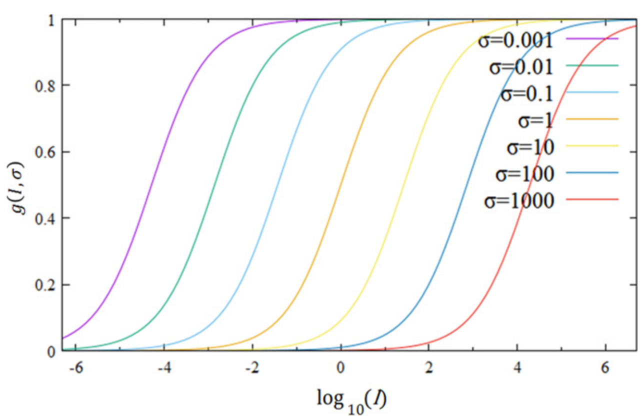

Figure 2. Retina response curves for each adaptation level σ of luminance.

2.1 *Retinal Response Model*

Numerous image-processing algorithms for improving the perceptual image quality when considering the human visual system have been developed. The most widely used is a retina response model defined by Naka and Rushton [10]. We also applied this model in the present study. In the equation used for the retinal response model developed by Naka and Rushton, the responses $g(I,\sigma)$ to the intensity of the incident light I are

$$g(I,\sigma) = \frac{R}{R_{\max}} = \frac{I^n}{I^n + \sigma^n}, \qquad (1)$$

where R ($0 < R < R_{\max}$) denotes the response of the photoreceptors, $R_{\max}$ denotes the maximum value of the responses, and I denotes the luminance value. The parameter σ takes the value of R when $R = 0.5 \times R_{\max}$, which corresponds to the adaptation level for the illumination. The parameter n is a sensitivity control exponent with a value between 0.7 and 1.0 in general [16]. Figure 2 shows the retinal response curves when the adaptation level σ varies from 0.001 to 1000 ($n = 0.7$). The retinal response follows a sigmoid curve and shifts when the adaptation level σ increases corresponding to the luminance level with the retina accepting more light energy.

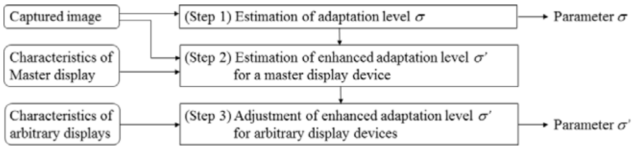

Figure 3. Estimation procedure.

2.2 *PuRet Algorithm*

The PuRet algorithm mimics the output image from the retina when an observer carefully gazes at the surface appearance of an object. We assume that images are captured using a digital color camera reproduced based on the Naka–Rushton retinal response model under adaptation level σ. This image is equivalent to the normal image shown in Fig. 1. As the pupil size contracting through careful observation, we suppose that the adaptation level σ increases by a level of σ' ($\sigma < \sigma'$). This hypothesis is reasonable because the contraction of the pupil size induces a false recognition that light of a stronger luminance and intensity is incident, resulting in a deterioration of the photoreceptor. Therefore, the conversion function φ is designed as follows:

$$g\left(I, \sigma'\right) = \varphi(g(I, \sigma)). \tag{2}$$

The parameter σ should be determined depending on the luminance of the actual scene, and the parameter σ' should be determined depending on both the amount the pupil diameter contracts and the characteristics of the reproduction display. However, in [9], it was necessary to manually adjust these parameters of PuRet as related to the retinal response for each scene and display device.

3. PARAMETER ESTIMATION MODEL

In this study, we propose an estimation model for both parameters σ and σ' from captured RAW image data. Figure 3 shows the procedure used in the estimation. In step 1, we estimate the adaptation level as the parameter σ from the captured scene. In step 2, we use a master display device and estimate the enhanced adaptation level as parameter σ' depending on both the amount of the pupil diameter contraction and the display device from the captured scene and display characteristics. In step 3, we adjust parameter σ' for an arbitrary display based on the characteristics of the display device.

3.1 *Estimation of Adaptation Level σ*

In step 1, we estimate the adaptation level as parameter σ from the captured scene. By correlating the radiance of a gray chart and the camera value beforehand, we can obtain the luminance for the actual scene in each pixel from the captured RAW image data. The problem is therefore how to estimate the adaptation level from the captured pixel-based luminance values. We conducted an experiment using a Canon EOS-1Ds Mark III as an example.

In our experiment, 100 high dynamic range (HDR) test scenes were captured by changing the chrominance and brightness of the illuminant for the scene shown in Figure 4.

Figure 4. HDR test scene (max: 52,726 cd/m^2; min: 940 cd/m^2; med: 5370 cd/m^2).

The test scenes consisted of objects with various factors of material appearance such as glossiness (metallic plates, a knife, and a spoon), translucency (a bottle of water and a glass), and roughness (stones, balls, and fruits). Here, both 14-bit RAW and 8-bit JPEG images for each color channel were output from the camera. In order to simply show the test scene, Fig. 4 represents a captured JPEG image. Actually, in this scene, we captured three types of 14-bit RAW images while doubling the exposure time and generated a 16-bit HDR image by the linearly synthesizing technique. Our objective was to estimate the adaptation level σ used when generating a JPEG image from the RAW image inside the camera. It was disclosed whether the Naka–Rushton retinal response model is used for this camera. However, because a nonlinear conversion of the luminance value is applied in all cameras, we assumed that it could be approximated using the Naka–Rushton retinal response model. The model was applied to a captured RAW image while changing the parameter σ, and the peak signal-to-noise ratio (PSNR) was calculated using the captured JPEG image. Parameter σ with the largest PSNR was then determined as the optimum σ for the scene.

Figure 5 shows the PSNR values for each parameter σ in a test scene. In general, when generating a JPEG image from a RAW image, various conversion processes other than the nonlinear luminance conversion are conducted. Therefore, although the PSNR value is too small, the unimodal results were confirmed. In this test scene, $\log(\sigma) = 4.16$ was the optimum value. We determined the optimum σ for the 100 different test scenes. Then, by analyzing the relationship between the optimum value σ and the luminance value of each test scene, we found that the optimum value σ was related to I_{median}, which is the median luminance value of all pixels in each test scene, as shown in Figure 6.

As shown in Fig. 6, the relationship between I_{median} calculated from the captured RAW images and the optimum parameters σ can be represented through a piecewise linear

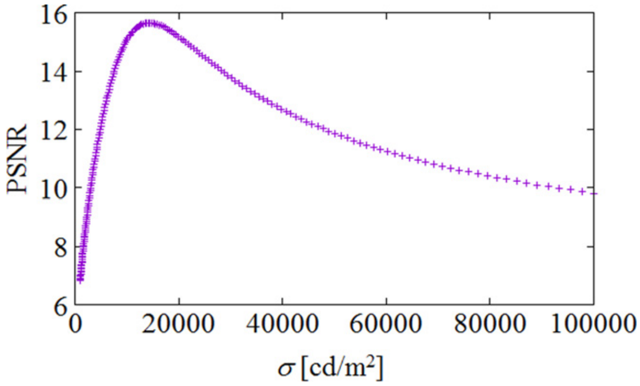

Figure 5. PSNR for σ in a test scene.

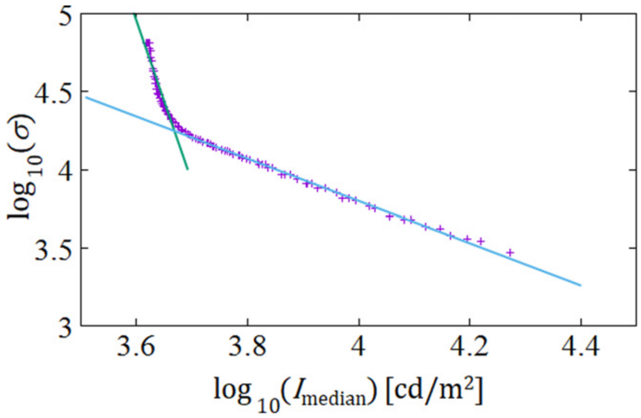

Figure 6. The relationship between the median luminance value of all pixels and the optimum σ for 100 different test scenes. The purple crosses indicate the test scenes, and two blue lines represent a piecewise linear approximation.

function as follows:

$$\sigma = \begin{cases} -10.3 \times \log_{10}(I_{\mathrm{median}}) + 42.2, & \log_{10}(I_{\mathrm{median}}) < 3.67 \\ -1.35 \times \log_{10}(I_{\mathrm{median}}) + 9.20, & \text{otherwise.} \end{cases} \tag{3}$$

The coefficient of determination of the estimated value σ for 100 test scenes is $R^2 = 0.987$. It should be noted that the estimation model in Eq. (3) depends on the camera characteristics and, therefore, needs to be derived for each specific camera in advance.

3.2 *Estimation of Enhanced Adaptation Level σ' for Master Display Device*

The parameter σ' indicates the variation in the amount of adaptation level σ based on the pupil dilation, which varies depending on the display characteristics. In this section, we first derive the enhanced adaptation level σ' experimentally under the fixed characteristics of a master display device.

Because σ' is the adaptation level of the perceived scene when focusing on the material appearance, it is originally determined through an appearance matching between the real scene and the reproduced image. However, when appearance matching was applied during the preliminary experiment, it caused mental stress in the subjects, and we therefore abandoned it for ethical reasons. Thus, in this study, we chose to determine σ', which is the reproduced image perceived to have the best material appearance, under the assumption that the image with such an appearance was the most preferred.

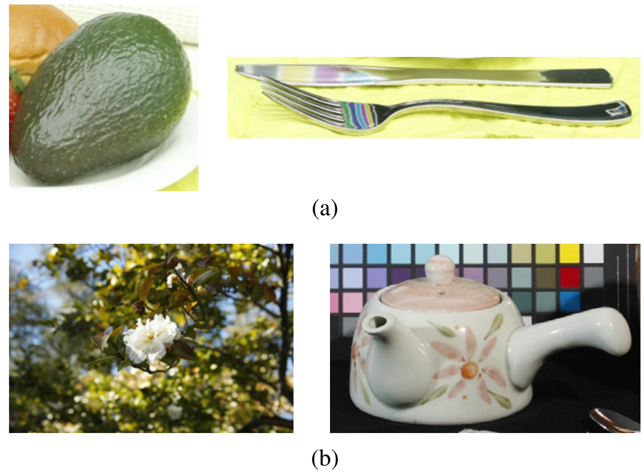

Figure 7. Test images used to determine the best material appearance. (a) Partial objects of the test scene shown in Figure 4. (b) New scenes.

In our experiment, 28 types of test images were prepared, namely 14 partial scenes obtained by cutting out the objects from the test scene shown in Fig. 4 and 14 new scenes. Example test images are shown in Fig. 7. Each subject observed the test images as reproduced on a master display device (EIZO ColorEdge CG277) in a dark room. The initial image was transformed based on the value of σ derived in the previous section. The subject was able to freely switch to images reproduced by different σ values through a button operation, and for each of the 28 types of test images, the reproduced image with the best material appearance was selected. The viewing distance was 70 cm, and the viewing angle of the long side of each test image was 8.1°. Three subjects with normal color vision participated in the experiment.

Figure 8 shows the rate of variability σ'/σ for I_{ave}, which is the average luminance values of the reproduced image on the master display device. The purple and green plots indicate the results of the 14 objects shown in Fig. 4 and the 14 newly used scenes, respectively. For the master display device, the relationship between σ'/σ and I_{ave} is expressed through the following equation:

$$\sigma'/\sigma = \begin{cases} 0.0016 \times I_{\mathrm{ave}} + 0.9, & I_{\mathrm{ave}} < 62.5 \\ 1.00, & \text{otherwise.} \end{cases} \tag{4}$$

The lower limit of the rate of variability is 1 based on the results of the mydriasis when all subjects focused on the surface appearance of the objects in [9]. The coefficient of determination for the 28 scenes was $R^2 = 0.576$.

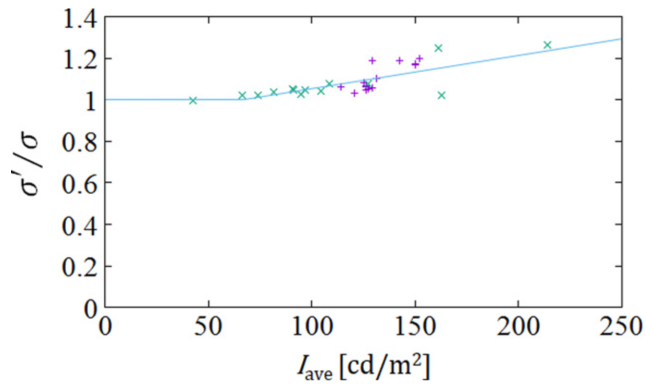

Figure 8. Rate of variability σ'/σ for the average of the luminance values of the master display device.

Table I. Display characteristics used in our additional experiments.

Display	Luminance (cd/m^2)		Contrast	Gamut
	Y_{Min}	Y_{Max}	Y_{Max}/Y_{Min}	
ColorEdge CG277 (Master display)	0.30	277	923	AdobeRGB
ColorEdge CG221	0.27	121	449	sRGB
ColorEdge CS230	0.34	253	743	sRGB
SHARP PN-A601	0.65	1914	2945	sRGB

3.3 *Adjustment of Enhanced Adaptation Level σ' for Arbitrary Display Device*

In general, it is conceivable that differences in the display characteristics affect the perception of the material appearance. For the appearance management on various display devices, we need to adjust the enhanced adaptation level depending on each display characteristic. Therefore, additional experiments were conducted using three displays with different characteristics to derive the rate of variability described for the master display device. Table I shows the display characteristics used in our experiments including the master display device. We measured the minimum (Y_{Min}) and maximum (Y_{Max}) luminance using a spectroradiometer (Konica Minolta, CS-2000) by setting $(R, G, B) = (1, 1, 1)$ and $(R, G, B) = (255, 255, 255)$, respectively. Here, due to the sensitivity of the spectroradiometer, we used $(R, G, B) = (1, 1, 1)$ as the minimum luminance. The display settings were default settings, and all optional functions such as local dimming were turned off.

The same psychophysical experiments for the master display were conducted. The same three subjects were the participants. Figure 9 shows the relationship between σ'/σ and I_{ave} for the three display devices. As with the master display device, the relationship can be approximated through piecewise linear functions. However, the slope of the function differed among the display devices, whereas the y-intercept remained almost constant at 0.9. The approximated functions shown in Fig. 9 are as follows:

(ColorEdge CG221)

$$\sigma'/\sigma = \begin{cases} 0.0036 \times I_{ave} + 0.9, & I_{ave} < 27.8 \\ 1.00, & \text{otherwise} \end{cases} \tag{5}$$

(ColorEdge CS230)

$$\sigma'/\sigma = \begin{cases} 0.0017 \times I_{ave} + 0.9, & I_{ave} < 58.9 \\ 1.00, & \text{otherwise} \end{cases} \tag{6}$$

(SHARP PN-A601)

$$\sigma'/\sigma = \begin{cases} 0.0003 \times I_{ave} + 0.9, & I_{ave} < 333.3 \\ 1.00, & \text{otherwise.} \end{cases} \tag{7}$$

The coefficients of determinations for 28 test scenes of the display devices shown in Figs. 9(a)–(c) were $R^2 = 0.581$, 0.598, and 0.495, respectively.

By investigating the slope and display characteristics, we found that there was a linear relationship between the logarithm of the display contrast and the slope of the function, as shown in Figure 10. The purple crosses indicate four displays, and the green line shows the linear approximation function.

The linear relationship can be represented as follows:

$$\text{Slope} = 0.0037 \times \log_{10}(Y_{max}/Y_{min}) + 0.013. \tag{8}$$

From the above, we can estimate the rate of variability σ'/σ by

$$\sigma'/\sigma = \begin{cases} \text{Slope} \times I_{ave} + 0.9, & \text{Slope} \times I_{ave} + 0.9 < 1.00 \\ 1.00, & \text{otherwise,} \end{cases} \tag{9}$$

and the enhanced adaptation level σ' for an arbitrary display device can be derived using the average scene luminance σ.

To verify the estimation model shown in Eq. (9), we prepared a new display device, an ASUS PA248Q, with the following characteristics: $Y_{min} = 0.25$, $Y_{max} = 286$, and $Y_{max}/Y_{min} = 1143$, using sRGB as the color gamut. The same additional experiment was conducted by the same three subjects. As shown in Figure 11(a), the relationship can also be represented through a piecewise linear function. We then plotted the slope onto Fig. 10, as indicated by the red circle in Fig. 11(b). We can confirm that the slope was estimated well for the unknown display device, which was not used to derive the estimation model.

To verify the feasibility of the proposed estimation model, we calculated the error of the estimated σ' by Eq. (9) and the value as evaluated by the subjects. Table II shows the root mean square error (RMSE) of $log_{10}\sigma'$ between the subjective and estimated values for the 28 test images. These results suggest that the RMSE is sufficiently small, and we can accurately manage the appearance of the material objects for arbitrary display devices.

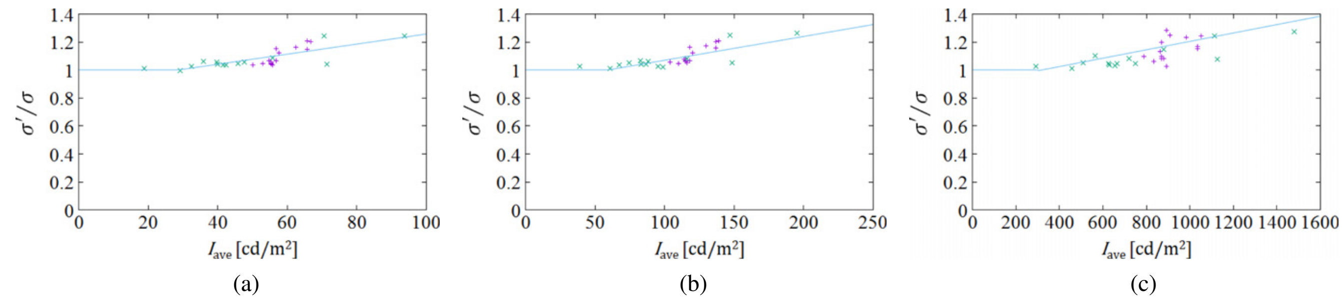

Figure 9. Rate of variability σ'/σ for the average of the luminance values of other displays. (a) Eizo ColorEdge CG221. (b) Eizo ColorEdge CS230. (c) SHARP PN-A601.

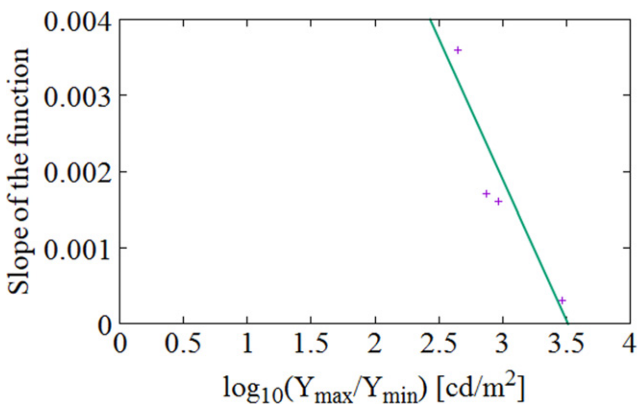

Figure 10. Linear relationship between the logarithm of the display contrast and the slope of the function.

Table II. RMSE of $log_{10}\sigma'$ between subjective value and the estimated value.

Display device	RMSE
ColorEdge CG277	0.074
ColorEdge CG221	0.050
ColorEdge CS230	0.084
SHARP PN-A601	0.107
ASUS PA248Q	0.050

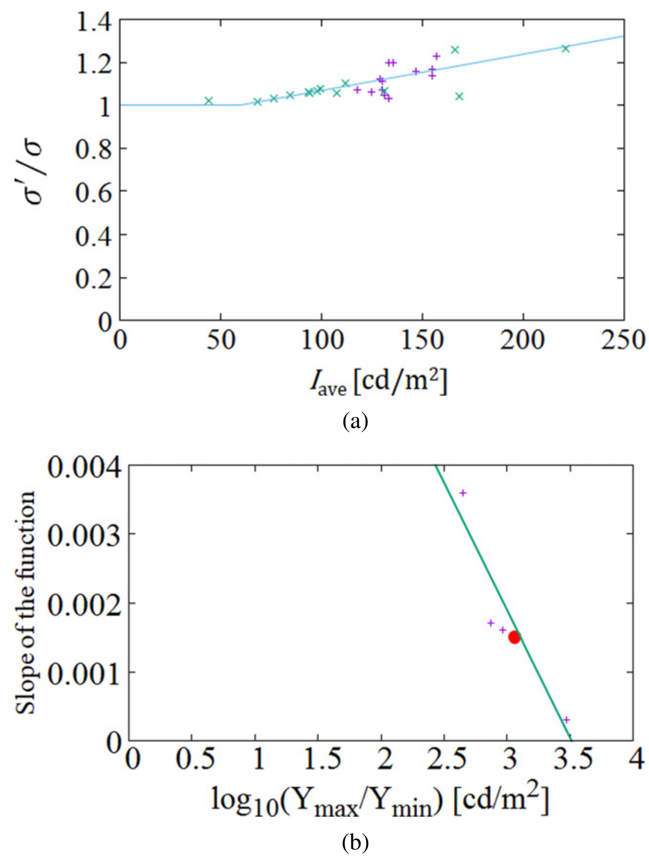

Figure 11. Estimated result for display device the ASUS PA248Q display device. (a) Rate of variability σ'/σ. (b) Estimated result of the slope of the function from the display contrast.

4. CONCLUSIONS

This study proposed a parameter estimation algorithm for two types of adaptation parameters used in our previously developed PuRet algorithm to realize the appearance management of material objects shown on a display device. We followed the concept of soft metrology and analyzed the physically measured values and the perceptual evaluations. Our results indicate that we succeeded in estimating an adaptation parameter from the median value of the scene luminance estimated from a RAW image. We also succeeded in estimating the other adaptation parameter from the average value of the scene luminance and the luminance contrast value of the output display device. As our contribution, it is possible to automatically generate an image that reproduces the perceived appearance when the material surface is carefully observed from RAW image data taken from a camera whose characteristics are known in advance. Furthermore, an automatic adjustment can be achieved based on the contrast characteristics, and thus the same appearance can be perceived regardless of the characteristics of the display device applied.

The parameter estimation used by the proposed method requires RAW image data. If we can estimate such information from existing JPEG data, the usefulness of the approach will be expanded. A parameter estimation from JPEG images will be an area of further study. Furthermore, we will verify the effectiveness of the proposed algorithm by comparing original scenes and the reproduced image on the display device by human viewer.

ACKNOWLEDGMENTS

This work was supported by Grant-in-Aid for Scientific Research on Innovative Areas (No. 15H05926) from MEXT, Japan.

REFERENCES

[1] R. W. Fleming, S. Nishida, and K. R. Gegenfurtner, "Perception of material properties (part I)," Vis. Res. **109, Part B**, 123–236 (2015).

[2] R. W. Fleming, S. Nishida, and K. R. Gegenfurtner, "Perception of material properties (part II)," Vis. Res. **115, Part B**, 157–302 (2015).

[3] M. Tanaka and T. Horiuchi, "Investigating perceptual qualities of static surface appearance using real materials and displayed images," Vis. Res. **115, Part B**, 246–258 (2015).

[4] J. B. Nielsen, H. W. Jensen, and R. Ramamoorthi, "On optimal, minimal BRDF sampling for reflectance acquisition," ACM Trans. Graph. **34**, 186 (2015).

[5] M. Aittala, T. Wwyrich, and J. Lehtinen, "Two-shot SVBRDF capture for stationary materials," ACM Trans. Graph. **34**, 110 (2015).

[6] J. Filip and R. Vávra, "Template-based sampling of anisotropic BRDFs," Comput. Graph. Forum **33**, 91–99 (2014).

[7] E. A. Khan, E. Reinhard, R. W. Fleming, and H. H. Bülthoff, "Image-based material editing," *Proc. ACM SIGGRAPH* (ACM, New York, NY, 2006), pp. 654–663.

[8] I. Boyadzhiev, K. Bala, S. Paris, and E. Adelson, "Bandsifting decomposition for image-based material editing," ACM Trans. Graph. **34**, 163 (2015).

[9] M. Tanaka, R. Arai, and T. Horiuchi, "PuRet: material appearance enhancement considering pupil and retina behaviors," J. Imaging Sci. Technol. **61**, 040401-1–040401-8 (2017).

[10] K. I. Naka and W. A. H. Rushton, "S-potential from colour units in the retina of fish (Cyprinidae)," J. Physiol. **185**, 587–599 (1966).

[11] J. C. Krynicki, "Introduction to 'soft' metrology: a CIE challenge of soft metrology," *18'th IMEKO World Congress Metrology for a Sustainable Development* (IOP Publishing, UK, 2006).

[12] G. B. Rossi and B. Berglund, "Measurement involving human perception and interpretation," Measurement **44**, 815–822 (2011).

[13] M. R. Pointer, "New directions soft requirements for support form mathematics, statistics and software," NPL Report CMSC20/03 (2003).

[14] CIE 175:2006 "A framework for the measurement of visual appearance," CIE Publication 175:2006, International Commission on Illumination, (2006).

[15] C. Eugène, "Measurement of Total visual appearance, a CIE challenge on Soft Metrology," *12th IMEKO TC1&TC7 joint Symposium on Man, Science and Measurement* (IOP Publishing, UK, 2008).

[16] J. E. Dowling, *The Retina: An Approachable Part of the Brain* (Belknap Press, Cambridge, Mass, USA, 1987).